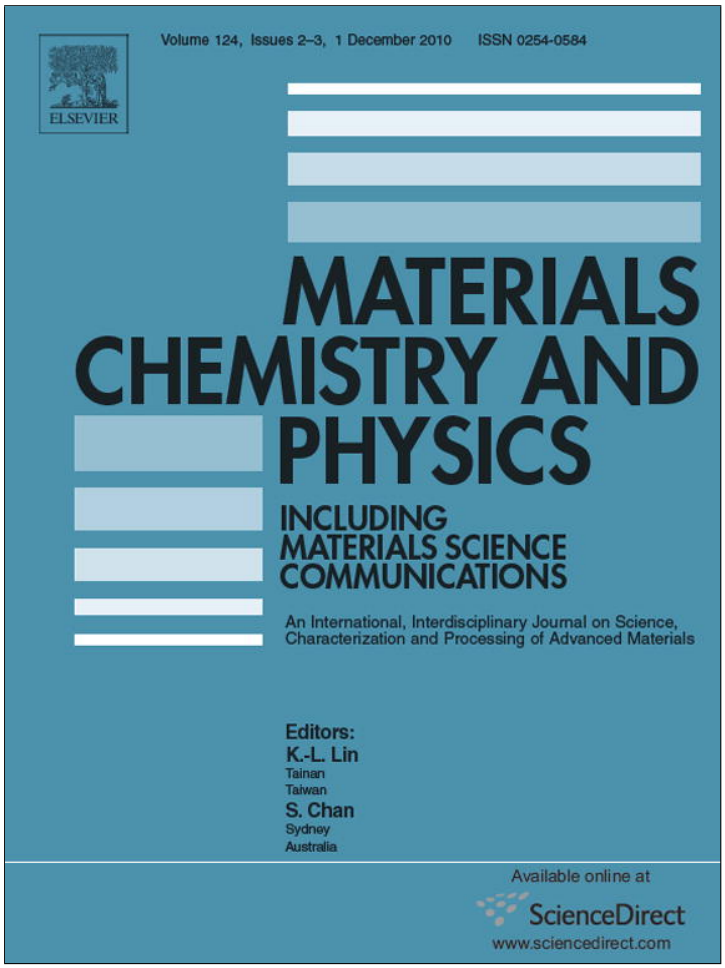

Materials Chemistry and Physics 124 (2010) 946–951

Contents lists available at ScienceDirect

Materials Chemistry and Physics

journal homepage: www.elsevier.com/locate/matchemphys

Synthesis under usual conditions, X-ray photoelectron spectroscopy and magnetic properties of $Re_{1-x}Mn_xO_2$ oxides with rutile structure

G.V. Bazuev[a,*], T.I. Chupakhina[a], A.V. Korolyov[b], M.V. Kuznetsov[a]

[a] Institute of Solid State Chemistry, Ural Branch of the Russian Academy of Sciences, 620990 Ekaterinburg, Russia
[b] Institute of Metal Physics, Ural Branch of the Russian Academy of Sciences, 620041 Ekaterinburg, Russia

ARTICLE INFO

Article history:
Received 26 March 2010
Received in revised form 1 July 2010
Accepted 25 July 2010

Keywords:
$Re_{1-x}Mn_xO_2$
Synthesis
Crystal structure
XPS spectra
Magnetic properties

ABSTRACT

Solid solutions $Re_{1-x}Mn_xO_2$ ($x = 0$; 0.08; 0.21) with a tetragonal rutile-type structure (sp. gr. $P4_2/mnm$, $z = 2$) have been synthesized from NH_4ReO_4, $KReO_4$ and $KMnO_4$ in argon atmosphere at 450–520 °C in a quartz cell. According to XPS measurements, Mn in solid solutions $Re_{1-x}Mn_xO_2$ is present as Mn^{3+} and Mn^{2+} cations, while the degree of oxidation of Re partly increases to penta- or hexavalent state. A transition of ReO_2 presumably in the antiferromagnetic state at 41 K was for the first time established by magnetic measurements. Along with the anomaly at 41 K, the second magnetic transitions at 6.5 K ($x = 0.08$) and 11 K ($x = 0.21$) was registered in these solid solutions.

1. Introduction

Re-containing solid solutions (SS) based on transition metal oxides with a rutile-like structure attract much attention in connection with a problem of search of new catalysts [1–3], and also in connection with possibility of synthesis of the ordered phases and compositions with multiple Re–Re bonds. To date, the following SS have been synthesized and examined: $Re_{1-x}Mo_xO_2$ ($0 < x < 0.37$ [4]), $A_{1-x}Re_xO_2$ (A = V, $x = 0.20$ [5]) and ARe_2O_6 (A = Cr, Fe, Co, Ni) [6,7]. SS A_2ReO_6 were obtained as a rule by high-pressure high-temperature synthesis. Depending on the temperature of synthesis, samples of the composition ARe_2O_6 (A = Ni, Fe, Co) crystallize either as phases with a tetragonal (high-temperature synthesis) or monoclinic and orthorhombic rutile structure (low-temperature synthesis) [6,7]. $CrRe_2O_6$ with an ordered trirutile structure and tetragonal and monoclinic modifications of $Re_{1-x}Cr_xO_2$ were obtained under similar conditions.

The compounds $AReO_4$, synthesized under high pressures forms an ideal rutile-type structure ($FeReO_4$, $AlReO_4$, $GaReO_4$) as well as orthorhomic rutile-type modification ($CoReO_4$ and $NiReO_4$). $MgReO_4$, $MnReO_4$ and $ZnReO_4$ crystallize in wolframite-type structures [8]. $V_{0.5}Re_{0.5}O_2$ phase produced under high pressures [9] has a rutile structure.

SS $Re_{1-x}Mo_xO_2$ (orthorhombic modification) were synthesized at ambient conditions by transport reactions method, while $V_{0.8}Re_{0.2}O_2$ (tetragonal structure) were produced in evacuated quartz tubes. The $Re_{1-x}Cr_xO_2$ phase ($0.31 < x < 0.44$) was obtained along with high-pressure high-temperature method also by decomposition of chrome hydrate perrhenate $Cr(ReO_4)_3 \cdot 6H_2O$ in dynamic vacuum at temperature 743–803 K with subsequent annealing in a quartz tube at 873–1423 K [6].

From this brief overview it is seen that the majority of Re-containing SS and rutile-structure compounds are characterized by a rather high content of the second element. No ReO_2-based SS having a small content of doping elements have been produced hitherto. This situation is explained by the consideration [10–12] that the rhenium dioxide ReO_2 has two modifications—monoclinic (the MoO_2-type structure (sp. gr. $P2_1/c$ [10]) and orthorhombic (the PbO_2-type structure (sp. gr. *Pbcn* [11]). If ReO_2 is synthesized at temperatures below ~350 °C, it has a monoclinic structure. This polymorphous form can be obtained by dehydration of $ReO_2 \cdot 2H_2O$ or by decomposition of ammonium perrhenate NH_4ReO_4. The monoclinic modification is characterized by the presence of metal–metal pairs (multiple bonds) along the *c* axis. The distance between coupled Re^{4+} cations is much smaller than between cations from different pairs. When the temperature increases above ~460 °C, the oxide undergoes an irreversible polymorphous transition in the orthorhombic modification. This structure is characterized by zigzag-like chains of Re-containing octahedra along the *c* axis. The high-temperature polymorph of ReO_2 in the pure form can be produced by decomposition of ammonium perrhenate at 650–670 °C by reaction:

$$2NH_4ReO_4 \leftrightarrow 4H_2O + N_2 + 2ReO_2 \quad (1)$$

* Corresponding author. Tel.: +7 343 374 4943; fax: +7 343 374 4495.
E-mail address: bazuev@ihim.uran.ru (G.V. Bazuev).

0254-0584/$ – see front matter © 2010 Elsevier B.V. All rights reserved.
doi:10.1016/j.matchemphys.2010.07.057

The process takes place in the atmosphere of dry nitrogen, argon or in vacuum.

Synthesis and electronic properties of the tetragonal modification of ReO_2 were reported in [13]. As distinct from the above-mentioned method of synthesis, here sodium perrhenate $NaReO_4$ was used as a Re-containing reagent. A mixture of $NaReO_4$ and ammonium chloride NH_4Cl taken in excess with respect to NH_4ReO_4 formation was annealed in He atmosphere in a quartz cell at temperatures from 300 to 450 °C for 4 h. It was found that the initial reagents practically did not interact in the temperature range 300–380 °C (as checked from the amount of condensed water at the cold cell end). At 420 °C, the reaction was rather intensive and terminated in 3–4 h. The powder-like reaction product was washed with distilled water to remove sodium chloride; then it was dried and analyzed. In contrast to decomposition of NH_4ReO_4, ReO_2 formed in this reaction had a rutile-type crystal structure with tetragonal symmetry. When the annealing temperature increased, reflections of the orthorhombic phase ReO_2 appeared on the X-ray diffraction pattern. At 600 °C, the sample consisted completely of the orthorhombic rhenium oxide ReO_2. According to [13], the tetragonal modification of ReO_2 (sp. gr. P42/mnm) has the following unit cell parameters: $a = 4.79825(5)$ Å, $c = 2.80770(4)$ Å, $V = 64.64$ Å^3, $c/a = 0.5852$.

It is interesting to use the technique [13] for production of tetragonal form of ReO_2 under usual conditions in synthesis of SS $Re_{1-x}M_xO_2$, where M-3d-elements. In this work we studied the possibility of synthesis of the tetragonal SS $Re_{1-x}Mn_xO_2$, investigated its structure, oxidation states of rhenium and manganese cations, as well as its magnetic properties. As shown in [14], the two-componential system on a basis Mn and Re oxides, modified by the activated carbon, is rather effective in reaction catalytic decomposition methanol on CO and H_2. By authors [14] it is established that catalytic activity increase occurs at including manganese and rhenium irons in various oxidative states.

2. Experimental

Ammonium chloride NH_4Cl, perrhenates NH_4ReO_4 and $KReO_4$ and $KMnO_4$ were used as initial reagents for synthesis of ReO_2 and solid solutions $Re_{1-x}Mn_xO_2$. The reactions were carried out in a quartz cell in argon atmosphere.

X-ray diffraction studies were performed in Cu Kα-radiation using a DRON-UM-1 diffractometer. X-ray diffraction patterns were processed by the full-profile Rietveld analysis with the FULLPROF-2007 software.

The products of synthesis were analyzed by mass spectrometry with inductively coupled plasma (mass spectrometer Spectromass 2000, Germany) and atomic emission spectrography (spectrograph STE-1, Russia).

The X-ray photoelectron spectroscopy (XPS) measurements were provided by VG ESCALAB MK II. Powder samples were applied on a two-sided conductive adhesive tape. The Mg Kα line (1253.6 eV) was used as exciting X-ray radiation without monochromator. The scanning step was 0.1 eV; the spectrometer resolution was calculated from the $Ag3d_{5/2}$ line with the analyzer transmission energy of 10 eV. The half-width of this line was 0.82 eV. The spectrometer was calibrated against the $Au4f_{7/2}$ line (84.0 eV); the sample charging was estimated from C1s (284.5 eV) spectra from natural hydrocarbon contaminations on the surface. The composition of complex oxides $Re_{1-x}Mn_xO_2$ was determined from Re4p, Mn2p and O1s lines with the use of calculated values of photoionization sections for these states [15].

Magnetic measurements were carried out on a MPMS-5-XL SQUID magnetometer produced by QUANTUM DESIGN. A powder-like sample of ~0.2 g was placed into a gelatine capsule. Measurements were performed in the temperature range 2–300 K at magnetic field intensity 0.5 and 5 kOe. Temperature versus magnetization M and susceptibility χ dependences were determined for two experiment modes: ZFC and FC. In the ZFC mode, a sample was cooled to 2 K, then magnetic field of a given intensity was applied, and magnetization was measured during heating. In the FC mode, measurements were performed when the sample was cooled. Magnetization M and static magnetic susceptibility $\chi = M/H$ were determined from of static magnetic moment measurements, while the real component of magnetic susceptibility χ' was found from dynamic magnetic susceptibility measurements at the amplitude value of alternating magnetic field to 4 Oe.

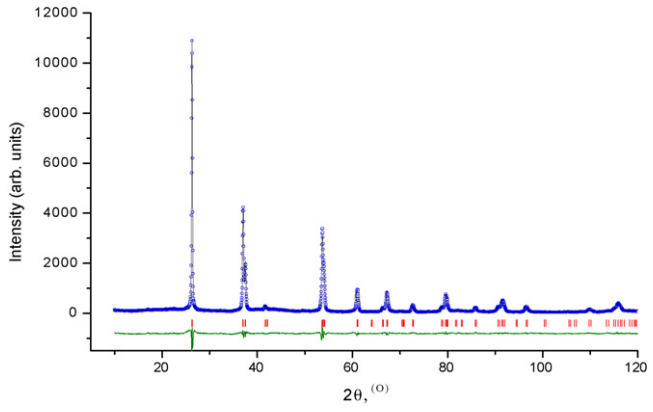

Fig. 1. Observed (circles), calculated (solid line) and difference (bottom line) X-ray powder diffraction patterns of $Re_{0.92}Mn_{0.08}O_2$.

3. Results

3.1. Synthesis and crystal structure

A reaction mixture of $KReO_4$, NH_4Cl and potassium permanganate $KMnO_4$ was annealed in a quartz cell in He atmosphere at 420 °C for 24 h, and then it was analyzed using X-ray diffraction. A phase with a rutile structure and KCl and $MnCl_2$ chlorides were found in the reaction products at 400–520 °C. KCl and $MnCl_2$ were separated by washing the obtained hard powder with twice-distilled water. Excess manganese, which did not enter into the composition of the solid phase, passed into the solution as Mn^{2+} cations and was quantitatively determined from manganese hydroxide precipitate formed when an alkaline solution was added.

According to spectral analysis, the content of Mn in the synthesized sample was 2.2 mass%, which corresponds to formula $Re_{0.92}Mn_{0.08}O_2$. Fig. 1 displays the observed, calculated and difference curves upon refinement by Rietveld method in the space group $P4_2/mnm$ for $Re_{0.92}Mn_{0.08}O_2$. It is seen that the calculated and experimental X-ray diffraction curves are in reasonable agreement, and therefore the rutile-type structure may be assigned to the considered complex oxide. This solid solution has a tetragonal rutile structure with parameters $a = 4.796(1)$, $c = 2.8263(2)$ Å, $V = 65.01$ Å^3, $c/a = 0.5893$, which differ from those of ReO_2 mainly owing to increased parameter c.

The synthesized solid solution $Re_{0.92}Mn_{0.08}O_2$ with the rutile structure is stable to 520 °C, whereas both tetragonal and monoclinic ReO_2 oxides partly transform in a rhombic modification at that temperature. When the temperature of annealing increases to 600 °C, in addition to the tetragonal phase, reflections of metallic rhenium appear on the X-ray diffraction pattern. The absence of a transition to the rhombic modification is indicative of the stabilizing effect of manganese on the tetragonal form.

The content of Mn in the solid solution $Re_{1-x}Mn_xO_2$ was increased by removing $KReO_4$ from the composition of the initial reagent. In the product of interaction of NH_4ReO_4 with $KMnO_4$ in argon atmosphere at 400–520 °C, the content of Mn was 6.5 mass%, which corresponds to $Re_{0.79}Mn_{0.21}O_2$.

The solid solution $Re_{0.79}Mn_{0.21}O_2$ has a rutile structure with the tetragonal cell parameters $a = 4.7843(2)$, $c = 2.8482(2)$ Å, $V = 65.19$ Å^3. Upon substitution of manganese for rhenium, the parameter a decreased (in comparison with the undoped sample and the solid solution $Re_{0.92}Mn_{0.08}O_2$), while the parameter c increased. The c/a ratio increased too: from 0.5852 for ReO_2 to 0.5953 for $Re_{0.79}Mn_{0.21}O_2$. Considering that for MnO_2 $c/a = 0.653$ [16], the observed increase in this ratio is a regular feature. All Re(Mn)–Re(Mn) distances along the c axis are equal and increase to 2.8482 Å as compared with the undoped oxide ReO_2 (for ReO_2 the Re–Re distance between the centers of octahedra is 2.8077 Å). The increase in the c/a ratio in comparison with the ideal value 0.58

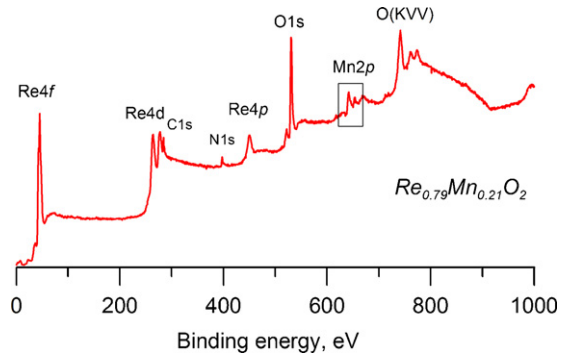

Fig. 2. Survey XPS spectrum of the solid solution $Re_{0.79}Mn_{0.21}O_2$.

[16] is indicative of attests to octahedra distortion. This gives rise to two groups of different Re(Mn)–O distances in the structure: 4 distances of 2.020(7) Å and 2 distances of 1.949(4) Å. Similarly to ReO_2 [13], octahedra in $Re_{0.79}Mn_{0.21}O_2$ are compressed along one axis. The octahedra distortion coefficient is 1.036. The mean Re(Mn)–O distance is 1.996 Å. The increase in the average Re–O distance from 1.989 Å in ReO_2 to 1.996 Å in $Re_{0.79}Mn_{0.21}O_2$ in spite of smaller ionic radius of Mn^{4+} cation (0.53 Å) than that of Re^{4+} (0.63 Å) [17], may be due to variation in the degrees of oxidation of Mn and Re. The parameter *x* for oxygen atom is 0.2870.

3.2. XPS analysis

X-ray photoelectron spectroscopy is widely used to study the electronic structure, chemical composition and degrees of oxidation of elements in examined materials. This method provides information about the thin surface layer of an examined sample, and therefore analysis of spectra makes it possible to conclude whether the surface composition corresponds to the composition of the substance.

XPS spectra of solid solutions $Re_{0.08}Mn_{0.92}O_2$ and $Re_{0.79}Mn_{0.21}O_2$ were used to estimate quantitative ratios Re/Mn and degrees of oxidation of these elements. Fig. 2 displays a survey XPS spectrum of the solid solution $Re_{0.79}Mn_{0.21}O_2$. The spectrum contains lines of photoelectron levels of rhenium, manganese and oxygen. In addition, a N1s line with binding energy 397.0 eV and a C1s line are also present in the spectrum. The appearance of nitrogen in the spectrum may be due either to the presence of decomposed ammonium perrhenate NH_4ReO_4 in the sample or to inclusion of nitrogen in the composition of the solid solution. The value of binding energy supports the supposition that nitrogen in the solid solution $Re_{0.79}Mn_{0.21}O_2$ is in the structurally bound state. It is significant that this line is also present in the spectrum of $Re_{0.08}Mn_{0.92}O_2$ (not shown). The C1s line attests to impurities on the surface of the powder.

XPS valence spectra of $Re_{0.92}Mn_{0.08}O_2$ and $Re_{0.79}Mn_{0.21}O_2$ are given in Fig. 3. As is seen, both samples have a non-zero electronic density at the Fermi level, which allows us to suppose metallic conductivity for these solid solutions. Fig. 4 exhibits Mn2p spectra of $Re_{0.08}Mn_{0.92}O_2$ and $Re_{0.79}Mn_{0.21}O_2$. On the basis of these spectra, we were going to obtain data on the oxidation state of Mn in these solid solutions. Note that the XPS method provides information on the surface layer of a sample, its composition, impurities and properties. However, in our study the content of Mn derived from XPS spectra and that found by chemical analysis are similar for both solid solutions. That is why XPS data allowed us to estimate the state of oxidation of manganese in the whole bulk of the sample.

According to findings [18,19], binding energy values for Mn2p increase with the oxidation state of this element if cations have the same coordination. The differences in the position of core

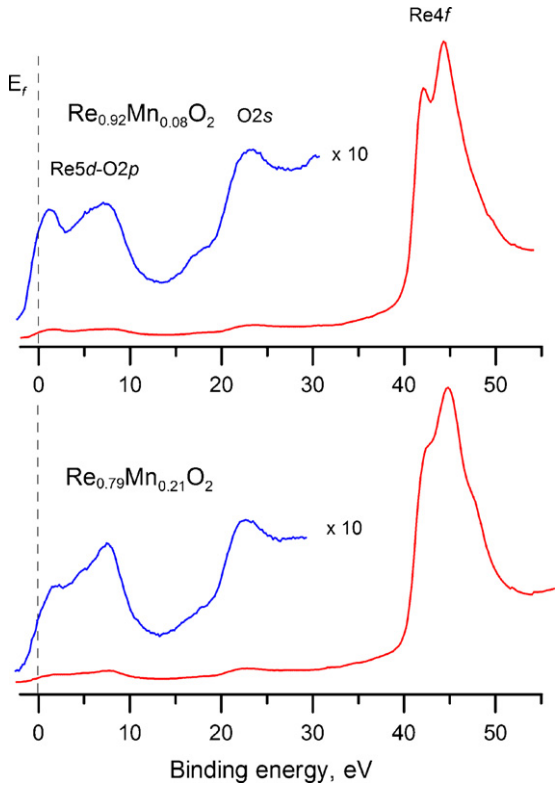

Fig. 3. XPS valence spectra of the solid solutions $Re_{0.92}Mn_{0.08}O_2$ and $Re_{0.79}Mn_{0.21}O_2$.

levels of Mn2p for Mn^{2+} and Mn^{3+} cations are insignificant (641.0–641.6 eV), whereas the core level of Mn^{4+} is between 642.0 and 642.6 eV. As follows from Fig. 4, the center of the $Mn2p_{3/2}$ peak for $Re_{0.08}Mn_{0.92}O_2$ is at 641.9 eV. Therefore, it may be concluded that Mn has predominantly intermediate valence Mn^{3+}–Mn^{4+}. In

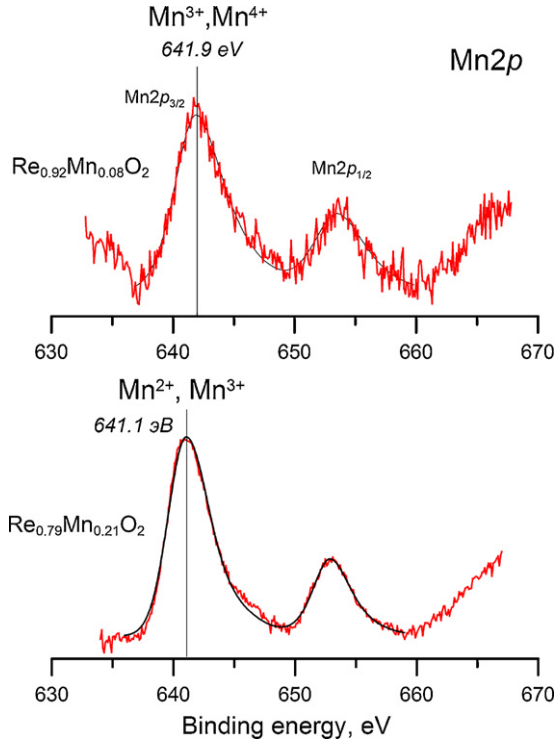

Fig. 4. Mn2p core-level spectra of $Re_{0.08}Mn_{0.92}O_2$ and $Re_{0.79}Mn_{0.21}O_2$.

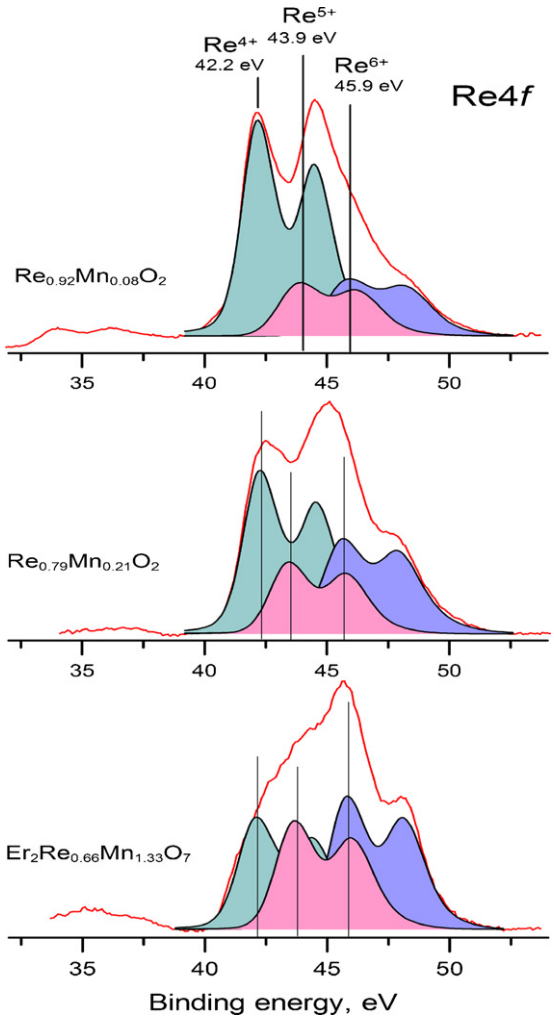

Fig. 5. Re4f core-level spectra of $Re_{0.92}Mn_{0.08}O_2$, $Re_{0.79}Mn_{0.21}O_2$ and $Er_2Re_{0.67}Mn_{1.33}O_7$.

$Re_{0.79}Mn_{0.21}O_2$, the center of the $Mn2p_{3/2}$ peak is displaced to 641.1 eV, which suggests a decrease in the average degree of oxidation of manganese. Probably, manganese in this solid solution is in the form of cations Mn^{2+} and Mn^{3+}.

Re4f XPS spectra of $Re_{0.08}Mn_{0.92}O_2$ and $Re_{0.79}Mn_{0.21}O_2$ are shown in Fig. 5. Similarly to Mn2p, positions of Re4f peaks shift to the high-energy region [20] as the oxidation state of rhenium increases. In conformity with data [3], the centers of $4f_{7/2}$ and $4f_{5/2}$ peaks for Re^{4+} cations are at 42.3 and 44.7 eV, respectively. For Re^{6+}, the first peak displaces to 45.3 eV, whereas the second peak shifts to 47.7 eV.

As follows from Fig. 5, XPS spectra of $Re_{0.08}Mn_{0.92}O_2$ and $Re_{0.79}Mn_{0.21}O_2$ are well described by the combination of three lines. Two of them represent a contribution from cations Re^{4+} (42.2 eV for $4f_{7/2}$) and Re^{6+} (45.9 eV for $4f_{7/2}$). The third line (43.9 eV for $4f_{7/2}$) reflects possibly the contribution of Re^{5+} cations. Unfortunately, we do not know any XPS spectra of compounds containing Re^{5+} cations. The information on synthesis of Re_2O_5 [21] was not confirmed later on (see [22]). At the same time there exist complex oxides, which formally contain Re^{5+} cation, for example, $La_5Re_3MnO_{16}$ [23], $Ln_2Mn_{2/3}Re_{4/3}O_7$ (Ln = Y, Er [24]), Ln_3ReO_7 [25], etc. As follows from comparison of intensities of lines corresponding to cations Re^{4+}, Re^{5+} and Re^{6+} (Fig. 5), $Re_{0.79}Mn_{0.21}O_2$ contains much more high-valence rhenium cations than $Re_{0.08}Mn_{0.92}O_2$. This situation is quite natural because the content of manganese characterized by a lower oxidation state increased. For comparison, Fig. 5c shows the Re4f XPS spectrum of $Er_2Mn_{2/3}Re_{4/3}O_7$, in which the oxidation states of Mn and Re are assumed to be +2 and +5, respectively. Similarly to $Re_{0.08}Mn_{0.92}O_2$ and $Re_{0.79}Mn_{0.21}O_2$, the observed spectrum is represented by lines corresponding to three different states of rhenium: Re^{4+}, Re^{5+} and Re^{6+}. Analysis of $Er_2Mn_{2/3}Re_{4/3}O_7$ spectra allows us to suggest disproportionation of Re^{5+} cations on Re^{4+} and Re^{6+} cations in this compound. Since the formal degree of oxidation here is +5, which is higher than in $Re_{1-x}Mn_xO_2$, the relative content of Re^{6+} in this compound is higher too.

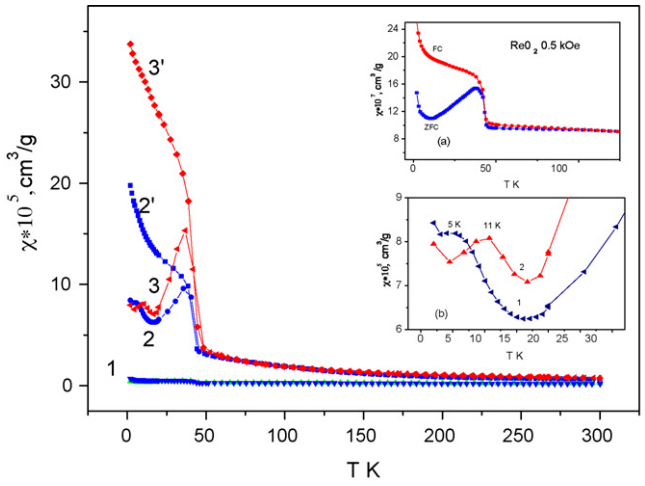

Fig. 6. Temperature dependences of magnetic susceptibility χ for ReO_2 (1), $Re_{0.92}Mn_{0.08}O_2$ (2—ZFC, 2′—FC) and $Re_{0.79}Mn_{0.21}O_2$ (3—ZFC, 3′—FC). The insets shows the ZFC and FC curves for ReO_2 (a), ZFC curves for $Re_{0.92}Mn_{0.08}O_2$ (b, curve 1) and $Re_{0.79}Mn_{0.21}O_2$ (b, curve 2) are enlarged for T near the magnetic transitions).

3.3. Magnetic properties

Temperature dependences of magnetic susceptibility χ for the tetragonal modification of ReO_2 and solid solutions $Re_{0.92}Mn_{0.08}O_2$ and $Re_{0.79}Mn_{0.21}O_2$ measured in the range 2–300 K in ZFC and FC modes in magnetic field 0.5 kOe are presented in Fig. 6. The $\chi(T)$ curves for ReO_2 in the inset (a) in Fig. 6 are given in a different scale for better visualization. Attention is drawn first of all to the increase in χ with the growth of the Mn content in the solid solutions, as well as to magnetic anomalies on all $\chi(T)$ curves at $T < 50$ K. All the samples demonstrate a considerable increase in susceptibility below ~50 K and appearance of divergency between the FC and ZFC curves at 40–45 K (for ReO_2, the FC and ZFC curves begin to diverge from 90 K). When measurements were performed in magnetic field of 5 kOe (not shown), susceptibility below 50 K also increased, but no divergency between the FC and ZFC curves for ReO_2 and $Re_{0.92}Mn_{0.08}O_2$ was observed, whereas for $Re_{0.79}Mn_{0.21}O_2$ this process takes place at 25 K.

For all the samples, the $\chi(T)$ dependences measured in magnetic field of 0.5 kOe in the ZFC mode exhibit maxima at ~42 K. When measurements were performed in magnetic field of 5 kOe, the maximum on the $\chi_{ZFC}(T)$ dependence was observed only for $Re_{0.79}Mn_{0.21}O_2$, which was displaced to 9 K. However, bends on the $\chi(T)$ curves in magnetic field of 5 kOe at about 40 K remained. As follows from Fig. 6, the $\chi_{ZFC}(T)$ dependences for $Re_{0.92}Mn_{0.08}O_2$ and $Re_{0.79}Mn_{0.21}O_2$ also exhibit maxima at 5 and 11 K, respectively.

When the temperature decreases, susceptibility measured in the FC mode increases over the whole temperature interval with a bend at 40 K.

Fig. 7 furnishes the results of dynamic (AC) χ' and χ'' susceptibility measurements, which confirm the presence of magnetic transitions in the examined samples: one for ReO_2 (at 41.5 K) and

Table 1
Magnetic properties of solid solutions $Re_{1-x}Mn_xO_2$.

Composition	$\chi_0 \times 10^6$ ($cm^3\,K\,mol^{-1}$)	θ (K)	C_{exp} ($cm^3\,K\,mol^{-1}$)	$C_{calc.}1$ ($cm^3\,K\,mol^{-1}$)	$C_{calc.}2$ ($cm^3\,K\,mol^{-1}$)	$C_{calc.}3$ ($cm^3\,mol^{-1}$)
$Re_{0.92}Mn_{0.08}O_2$	184	−0.69	0.232	0.15	0.24	0.35
$Re_{0.79}Mn_{0.21}O_2$	225	−12	0.37	0.394	0.63	0.92

two transitions for solid solutions $Re_{0.92}Mn_{0.08}O_2$ (at 41 and 6.5 K) and $Re_{0.79}Mn_{0.21}O_2$ (at 41 and 11 K). AC (χ') susceptibility of ReO_2 was measured at different frequencies (100, 1000 and 10000 Hz) with the amplitude value of alternating magnetic field to 4 Oe. As is seen from the inset (a) in Fig. 7 (data only for 100 and 10,000 Hz are shown), the position of the maximum at 41.5 K does not change with frequency f, whereas the value of χ' decreases as f increases.

Magnetization versus applied magnetic field dependences at 2 K for all the samples have a nonlinear character and are characterized by hysteresis and the absence of saturation in magnetic fields to 30 kOe. Data for ReO_2 and $Re_{0.79}Mn_{0.21}O_2$ are presented in Figs. 8 and 9 respectively.

Fig. 10 demonstrates temperature dependences of the inverse magnetic susceptibility χ for the solid solutions $Re_{0.92}Mn_{0.08}O_2$ and $Re_{0.79}Mn_{0.21}O_2$ in magnetic field of 5 kOe. Both dependences obey the modified Curie–Weiss law

$$\chi = \chi_0 + \frac{C}{T-\theta},$$

where χ_0 is the temperature-independent component of magnetic susceptibility, $cm^3\,mol^{-1}$, C is the Curie constant, $cm^3\,K\,mol^{-1}$, and θ is the Weiss temperature, K. Table 1 lists the Curie–Weiss equation parameters and χ_0 values. From these data it follows that the constant θ becomes more negative and the values of the Curie constant and χ_0 increase when the content of Mn grows.

The calculated values of the Curie constant are given in Table 1 for three versions of cation combinations: Mn^{4+}–Re^{4+} ($C_{calc.}1$), Mn^{3+}–Re^{5+}, Re^{4+} ($C_{calc.}2$) and Mn^{2+}–Re^{4+}, Re^{5+} or Re^{6+} ($C_{calc.}3$). Here it was assumed that the 3d electrons of manganese are localized, while the 5d electrons of rhenium are collectivized.

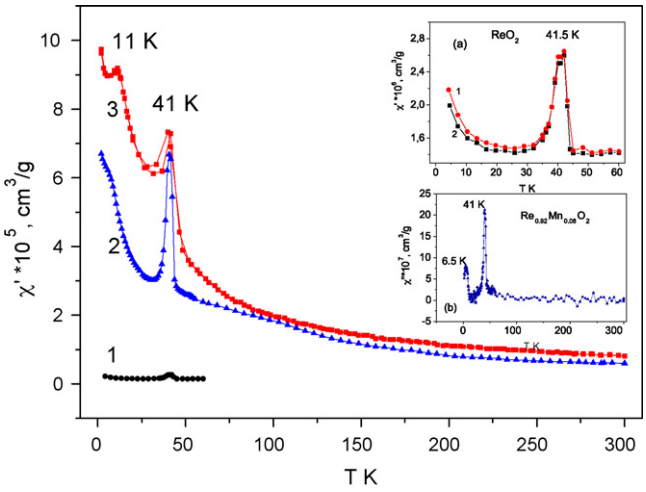

Fig. 7. Temperature dependence of dynamic magnetic susceptibility χ' for ReO_2 (1), $Re_{0.92}Mn_{0.08}O_2$ (2) and $Re_{0.79}Mn_{0.21}O_2$ (3). The insets shows the dependences of $\chi' = f(T)$ for ReO_2 (a, 1—f = 100 Hz, 2—f = 10,000 Hz) are enlarged for χ' near magnetic transition and χ'' (b) for $Re_{0.92}Mn_{0.08}O_2$.

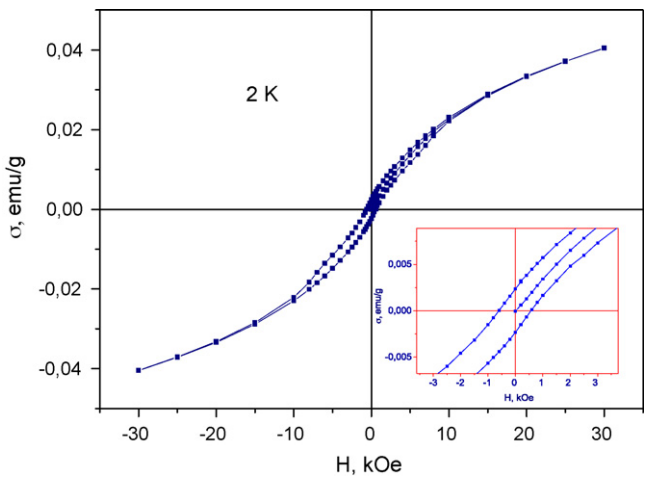

Fig. 8. Magnetization versus applied magnetic field for ReO_2 at 2 K.

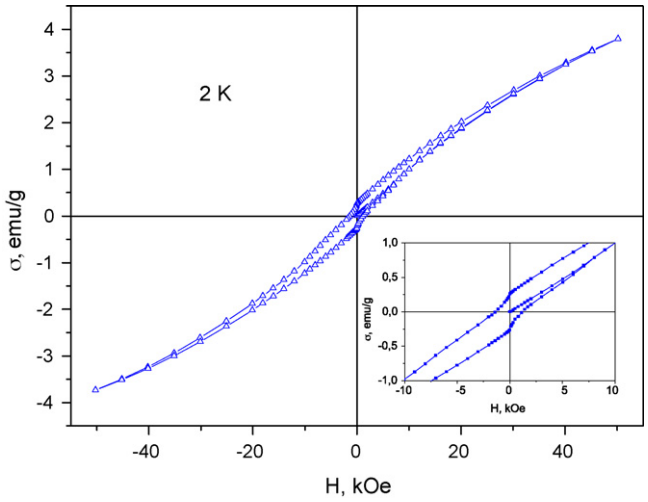

Fig. 9. Magnetization versus applied magnetic field for $Re_{0.79}Mn_{0.21}O_2$ at 2 K.

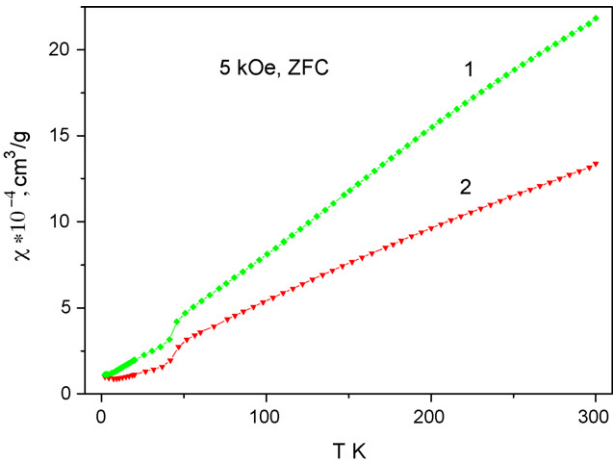

Fig. 10. Temperature dependences of inverse magnetic susceptibility χ for (1) $Re_{0.08}Mn_{0.92}O_2$ and (2) $Re_{0.79}Mn_{0.21}O_2$.

4. Discussion

The electric and magnetic properties of transition metal oxides with the rutile structure are determined both by the peculiarities of their structure and the electronic configuration of d elements. In the rutile structure, transition metal cations form a body-centered tetragonal lattice and are located in octahedral environment of oxygen anions. The octahedra filled with cations share an edge along the *c* axis, in the direction of which chains of octahedra and direct cation–cations bonds are formed. The chains are joined through octahedra vertices and form a three-dimensional structure. This structure is favorable also for cation–anion–cation interactions [12] and allows compounds to exhibit metallic conductivity in addition to semiconducting conductivity.

Pressed polycrystalline samples of β-MnO_2 having a tetragonal rutile structure manifested semiconducting properties [12]. The β-MnO_2 monocrystal displays metallic conductivity along the *c* axis below room temperature with a jump in electrical resistance in the Neel point (94 K), which drops sharply at $T < 94$ K [26]. Below this temperature, magnetically ordered antiferromagnetic state of helical type is formed.

Below 50 K, electric conductivity of MnO_2 increases again as the temperature lowers. The n-type metallic conductivity of MnO_{2-x} is due to crystal nonstoichiometry ($x = 0.027$). Magnetic susceptibility measurements on monocrystals revealed a considerable deviation from the model of localized electrons. Magnetic susceptibility of β-MnO_2 in the range 300–700 K follows the Curie–Weiss law with the Curie constant $C = 2.46\ \mathrm{cm^3\ K\ mol^{-1}}$ and the Weiss constant $\Theta = -783$ K. The value of C_{exp} is much greater than C_{theor} ($1.857\ \mathrm{cm^3\ K\ mol^{-1}}$). Measurements of χ for monocrystals coincide on the whole with the data obtained for polycrystalline samples [27] and are indicative of strong correlation between conduction e_g electrons and magnetic t_{2g} electrons.

In spite of essential differences in the structure, the orthorhombic and monoclinic modifications of ReO_2 display Pauli paramagnetism and metallic conductivity [12]. Note that magnetic susceptibility of ReO_2 [28] was measured in the interval 77–300 K for the orthorhombic modification and in the interval 85–300 K for the monoclinic modification.

The electronic and magnetic properties of ReO_2 with the rutile structure were studied by calculating its band structure in the LDA and LDA + U approximations [13]. It was found that antiferromagnetic ordering in ReO_2 is more favorable than ferromagnetic ordering. The calculated magnetic moment on Re atom is 1.0 μ_B. The calculations performed showed that ReO_2 exhibits both a metallic and covalent character with pronounced hybridization of O2p and Re5d states and a high degree of covalence of the Re–O bond.

The results of experimental investigations of magnetic properties of the rutile-structure oxide ReO_2 (Figs. 6–8) agree with the above conclusions. It may be supposed that the magnetic anomaly at ~41 K (Figs. 6 and 7) corresponds to the transition of ReO_2 in the antiferromagnetic ordered state. The discrepancy between ZFC and FC magnetic susceptibility below 90 K is not clear now. The non-linear dependence of magnetization on applied magnetic field at 2 K (Fig. 8) attests to a weak ferromagnetic moment and a canted magnetic structure. It is significant that the magnetic transformation point at 41 K is not virtually displaced when Mn is substituted for Re. At the same time, the second magnetic transition appears at lower temperatures: 6.5 K for $Re_{0.92}Mn_{0.08}O_2$ and 11 K for $Re_{0.79}Mn_{0.21}O_2$, which are likely to be connected with magnetic ordering of the subsystem of Mn–Re cations. It is noteworthy that the magnetic properties of $Re_{1-x}Mn_xO_2$ are similar on the whole to those of $Ni_{0.33}Re_{0.67}O_2$, which is ordered at 23.5 K in a phase with a ferromagnetic component, and of $Co_{0.33}Re_{0.67}O_2$, which is characterized by two magnetic transitions (at 27 and 17.5 K) [7].

Multi-valence states of Mn and Re found in $Re_{1-x}Mn_xO_2$ also agree with the data of work [7], in which XPS spectra of $Re4f_{7/2}$ and $Re4f_{5/2}$ and magnetic properties of rutile-structure solid solutions $M_{0.33}Re_{0.67}O_2$ (M = Fe, Co, Ni) are studied. According to XPS measurements, the Co- and Ni-containing phases contain a mixture of Re^{4+}/Re^{6+} and M^{2+}/M^{3+} cations.

The considerable deviation of the experimental Curie constant C_{exp} for $Re_{0.79}Mn_{0.21}O_2$ from C_{theor} calculated in the assumption that manganese in the solid solution is in the form of Mn^{3+} and Mn^{2+} cations can be explained by partial delocalization of t_{2g} electrons of manganese. This inference is also supported by the high value of the temperature-independent component of magnetic susceptibility ($1.2 \times 10^{-3}\ \mathrm{cm^3\ mol^{-1}}$) and by high electric conductivity of this sample. Considering this problem, we took into account that the replacement of Re^{4+} cations by Mn^{4+} cations in $Re_{1-x}Mn_xO_2$ is unlikely. So, in the high-pressure compound $MnReO_4$ with the wolframite structure [29] and in the perovskite Ba_2MnReO_6 [30], the degrees of oxidation of Mn and Re were found to be +2 and +6, whereas in $Y_2Mn_{2/3}Re_{4/3}O_7$ [24] they were +2 and +5, respectively.

References

[1] N. Escanola, J. Ojeda, R. Gid, G. Alves, A. Lopes Agudo, J.L.G. Fierro, F.J. Gil-Llambias, Appl. Catal. A: Gen. 234 (2002) 45.
[2] A. Kuzmin, J. Purans, E. Cazanelli, C. Vinegoni, G. Mariotto, J. Appl. Phys. 84 (1998) 5515.
[3] Y. Yuan, T. Shido, Y. Iwasava, Chem. Commun. (2000) 1421.
[4] J. Feller, H. Oppermann, R. Kucharkowski, S. Dabritz, Zeitschrift fur naturforschung. Section B—J. Chem. Sci. 53 (1998) 397.
[5] B.-O. Marinder, A. Magneli, Acta Chem. Scand. 12 (1958) 1345.
[6] D. Mikhailova, H. Ehrenberg, D. Tpots, G. Brey, S. Oswald, H. Fuess, J. Solid State Chem. 182 (2009) 1506.
[7] D. Mikhailova, H. Ehrenberg, S. Oswald, D. Tpots, G. Brey, H. Fuess, J. Solid State Chem. 182 (2009) 364.
[8] A.W. Sleight, Inorg. Chem. 14 (1975) 597.
[9] K.G. Bramnik, H. Ehrenberg, R. Theissmann, H. Fuess, E. Moran, Z. Kristallogr. 218 (2003) 455.
[10] S. Tribalot, M.L. Jungfleisch, D. Delafosse, C. R. Seances Acad. Sci. (Paris) 259 (1964) 210.
[11] A. Magneli, Acta Chem. Scand. 9 (1955) 28.
[12] D.B. Rogers, R.D. Shannon, A.W. Sleight, J.L. Gillson, Inorg. Chem. 8 (1969) 841.
[13] A.L. Ivanovskii, T.I. Chupakhina, V.G. Zubkov, A.P. Tyutyunnik, V.N. Krasilnikov, G.V. Bazuev, S.V. Okatov, A.I. Lichtenstein, Phys. Lett. A 348 (2005) 66.
[14] T. Tsoncheva, S. Vankova, O. Bozhkov, D. Mehandiev, Can. J. Chem. 85 (2007) 118.
[15] J.H. Scofield, J. Electron. Spect. Relat. Phenom. 8 (1979) 129.
[16] A.F. Wells, Structural Inorganic Chemistry, Oxford University Press, Oxford, England, 1986.
[17] R.D. Shannon, Acta Cryst. A 32 (1976) 751.
[18] J.L. Gautier, E. Rios, M. Gracia, J.F. Marco, J.R. Gancero, Thin Solid Films 311 (1997) 51.
[19] B. Murugan, A.V. Ramaswamy, D. Srinivas, C.S. Gopinath, V. Ramaswamy, Chem. Mater. 17 (2005) 3983.
[20] A. Cimino, B.A. De Angelis, D. Gazzoli, M. Valigi, Z. Anorg. Allg. Chem. 460 (1980) 86.
[21] L.V. Borisova, D.I. Ryabchikov, T.I. Yarinova, Zh. Neorg. Khim. 13 (1968) 321.
[22] T. Hartmann, H. Ehrenberg, G. Miehe, T. Buhrmester, G. Wltschek, J. Galy, H. Fuess, J. Solid State Chem. 160 (2001) 317.
[23] C.R. Wiebe, A. Gourrier, T. Langet, J.F. Britten, J.E. Greedan, J. Solid State Chem. 151 (2000) 31.
[24] G.V. Bazuev, T.I. Chupakhina, A.V. Korolyov, J. Alloys Compd. 486 (2009) 88.
[25] Y. Hinatsu, M. Wakeshima, N. Kawabuchi, N. Taira, J. Alloys Compd. 374 (2004) 79.
[26] H. Sato, T. Enoku, M. Izobe, Y. Ueda, Phys. Rev. B 61 (2000) 3563.
[27] N. Ohama, Y. Hamaguchi, J. Phys. Soc. Jpn. 30 (1971) 1311.
[28] P. Gibart, C. R. Acad. Paris 259 (1964) 4237.
[29] K.G. Bramnik, H. Ehrenberg, S. Buhre, H. Fuess, Acta Cryst. B61 (2005) 246.
[30] G. Popov, M. Greenblatt, Phys. Rev. B67 (2003) 024406.